Formation of SiC Rods in Composites of $SiC/SiO_2/C$ from Carbonized Wood Infiltrated with Ethylsilicate-40

Joko Sulistyo, Toshimitsu Hata, and Sri Nugroho Marsoem

Abstract

Silicon carbide rods were formed in composites of silicon carbide/silicon dioxide/carbon ($SiC/SiO_2/C$) from carbonized wood impregnated with ethyl silicate-40 after heat treatments using a pulse current apparatus. The effect of reaction temperatures, heating rates and pressures on the SiC rods formation was investigated. Raman spectroscopy indicated that the SiC rods possessed well crystalline. The SiC rods in the composites prepared at 1200 and 1400°C exhibited straight structure with smooth surfaces. The increase of reaction temperature up to 1600°C increased the length and diameter of SiC rods which exhibited a camelback-type structure. Different heating rate only determined the length of SiC rods grown; meanwhile the increase of pressure from 0 to 15 MPa increased the length and diameter of SiC rods grown.

Key words: SiC rod; $SiC/SiO_2/C$ composite; heat treatment; pulse current apparatus.

Introduction

Considerable interest has developed in the use of wood-based carbon material as a new source of carbon for engineering applications such as for electromagnetic shielding (Wang and Hung 2003), adsorbent of heavy metals from aqueous solution (Pulido *et al*. 1998), fire retardant material (Subyakto *et al*. 2000), thermal management in space solar power satellite (Sulistyo *et al*. 2009), electrical and thermal conductive material (Sulistyo *et al*. 2010), etc. Recently, it has been demonstrated that nano-materials such as silicon carbide (SiC) nanorods or nanowires could be grown inside the vessels of carbonized wood (Hata *et al*. 2005; Cheung and Ng 2007). The SiC nanorod have been focus of researches because they exhibit superior properties such as very high bending strength and Young's modulus (Zhu *et al*. 2005), an exceptional optical feature i.e. blue range photoluminescence emission (Gao *et al*. 2001), high chemical and thermal stabilities (Fan *et al*. 2006). Various fabrication methods were used to form nano SiC rod including sol-gel method (Hata *et al*. 2005; Cheung and Ng. 2007), nanotube confining growth, carbothermal reduction, chemical vapor deposition, laser ablation and chemical vapor infiltration (Zhu *et al*. 2005).

In this study, a simple sol-gel method was developed to grow SiC rods possessing different morphologies and dimensions in composites of $SiC/SiO_2/C$ by various heat treatments using a pulse current apparatus. The pulse current apparatus promotes a fast heat treatment in which the reaction temperature can be achieved in a short time. As the current passes through the graphite dies as well as through the sample, the sample is heated from both the inside and outside at the same time (Fujisawa *et al*. 2005). Moreover, the temperature, heating rate and pressure in the pulse current apparatus can be simply controlled. The purpose of this study was to investigate the formation of SiC rods related to the heat treatment conditions including reaction temperatures, heating rates and pressures. Mostly previous studies determined the mechanism of SiC rods formations and their microstructure (Hata *et al*. 2005; Cheung and Ng 2007). Until now, there has been no study on the heat treatments governing the growth and morphology of SiC rods. The morphology of SiC rods grown in composite of $SiC/SiO_2/C$ was observed by scanning electron microscope. The crystal phase of the composite and the crystal structure of SiC rods were analyzed by X-ray diffraction and Raman spectroscopy, respectively.

Materials and Methods

Sugi (*Cryptomeria japonica*) wood particles were heated at a rate of 4°C/min up to 700°C in a laboratory scale electric furnace. The particles were held at 700°C for 1 h under a N_2 gas flow of 100 mL/min. The resulting carbonized wood was then granulated using a blender and sieved to yield particle size of 45~150 μm. A silica solution was prepared by diluting ethylsilicate-40 (Colcoat, Japan) with ethyl alcohol to obtain a 15% SiO_2 concentration by weight. Carbonized wood was submerged in the silica solution and held under a vacuum of 1 kPa for 90 min. The carbonized wood infiltrated with ethylsilicate-40 was then preheat-treated at 100°C in an electric oven to cause the SiO_2 to be in a liquid phase. The final SiO_2 content calculated by the molar ratio was found to be 50% based on the dry charcoal weight. A dry weight of 1 g of carbonized wood infiltrated with SiO_2 was then placed into a 10 mm-internal-diameter graphite die with a length of 5 cm equipped with two graphite dies with a total length of 4.5 cm. Graphite punches with a total length of 5 cm were used in the heat treatments under 15 and 40 MPa. To evaluate the effect of reaction temperature, porous $SiC/SiO_2/C$ composites prepared with the carbonized wood infiltrated silica were heated to 1200, 1400 and 1600°C at a rate of 250°C/min under a pressure of 0 MPa. To evaluate the effect of heating rate, the carbonized wood infiltrated with

silica was heated at rates of 100 and 500°C/min up to 1400°C under a pressure of 0 MPa. To evaluate the effect of pressure, the carbonized wood infiltrated with silica was heated at rate of 250°C/min up to 1400°C under pressure of 15 and 40 MPa. All the heat treatments were used a reaction time of 30 min under a N_2 gas flow of 1 L/min using a pulse current sintering device (VCSP II, SS Alloy, Hiroshima). The resulting 5-mm-thickness samples were cut into discs with a thickness of approximately 0.8 mm.

X-ray diffraction (XRD, Rigaku-RINT-ultra X18) at 45 kV and 200 mA was used to determine the crystalline phase formed during sintering. The data were collected as continuous scans, with a step size of 0.02° 2θ and a scan rate of 1° 2θ/min between 10 and 90° 2θ. The bulk samples were analyzed without powdering since a random orientation of crystallites was assumed to be already present (Klett *et al*. 2004).

The microstructure of the samples was analyzed using Raman spectroscopy (Renishaw inVia) with an air-cooled CCD detector. An argon laser with a wavelength of 514.5 nm was used as an excitation source. The spectra were measured in the 600~1800 cm^{-1} range. Seven 10 sec accumulations were found to give an adequate signal-to-noise ratio. The wave number was calibrated using the 520 cm^{-1} line of a silicon wafer. Spectral processing was performed using WiRE 2 software.

Results and Discussion

Morphology of Carbonized Wood

Figure 2(a-b) shows the SEM images of carbonized wood particle which maintained the cellular structure as in the original wood. Lumens did still exist in the carbonized wood particle (point A in Figure 2a). SiO_2 in liquid phase covered the surface of carbonized wood particle after preheat treatment at 100°C, as shown in Figure 2(b), and infiltrated the lumens in the particle (point B in Figure 2b).

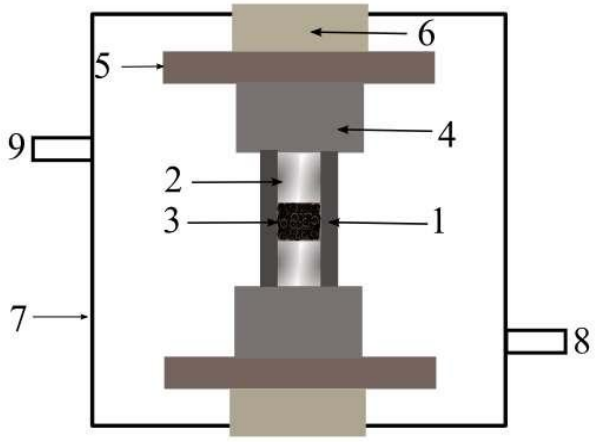

Figure 1. Schematic of a pulse current sintering apparatus: 1, graphite die; 2, graphite punch; 3, sample; 4, graphite bar; 5, graphite plate; 6, copper plate; 7, chamber; 8, pyrometer; 9, vacuum pump. The morphology of carbonized wood particles and composites samples was observed using scanning electron microscopy (SEM, JEOL-JSM-5310). The samples were observed directly without any coating.

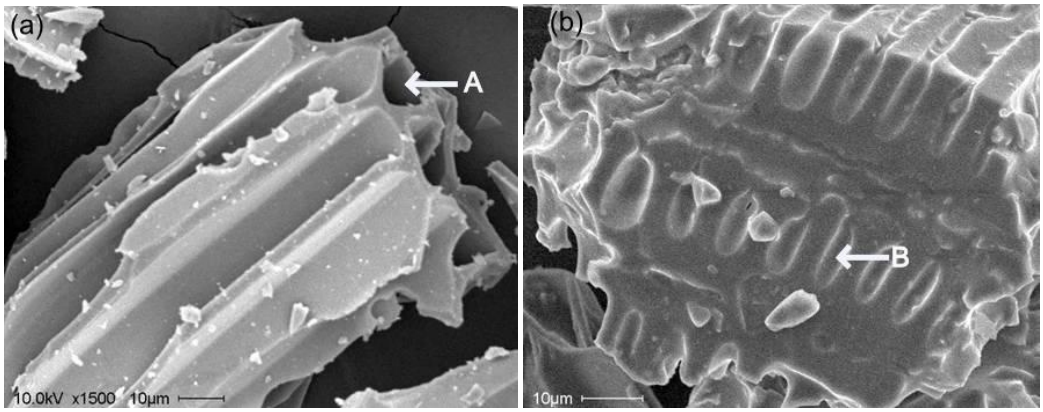

Figure 2. SEM images showing (a) the morphology of a carbonized wood particle and (b) a carbonized wood covered with SiO_2 in liquid phase after pre-heat treatment at 100°C.

Microstructure of the Composite Materials

The XRD pattern of composites of SiC/SiO_2/C prepared at different reaction temperatures are shown in Figure 3. Major diffraction peaks are observed at around 2θ = 14 and 17°, corresponding to the SiO_2 glass crystal phase, around 2θ = 26, 44 and 79°, corresponding to the (002), (101) and (110) turbostratic carbon phase, respectively, and around 2θ = 35, 42, 60 and 72°, corresponding to the (111), (200), (220) and (311) reflections, respectively, of the cubic β-SiC phase (Nakashima and Harima 1997; Vyshnyakova *et al*. 2006; Li *et al*. 2007; Senthil and Yong 2008). The intensity of β-SiC peaks in composite of SiC/SiO_2/C showed little dependence on the reaction temperatures. As the reaction temperature was similar, i.e. 1400°C, the heating rate and pressure showed less effects on the intensity of β-SiC peaks, as shown in Figure 4(a-b). However, the reaction at that temperature with a heating rate of 250°C/min (Figure 4a) and a pressure of 0 MPa (Figure 4b) gave slightly strong SiC peaks which were indicated a better SiC formation.

Ethylsilicate which was physically infiltrated in the carbonized wood particles as shown in Figure 2(b) vaporized at temperature of 100°C. The solution slowly decomposed into SiO_2 and other components by thermal decomposition. The reaction was given by (Cheung and Ng 2007):

$$Si(OC_2H_5)_4\ (l) \rightarrow SiO_2\ (l) + 4C_2H_4\ (g) + 2H_2O\ (g) \quad (1)$$

where *l* or *g* indicated that the component was in the form of liquid or gas. SiC were produced by the silica carbothermal reduction; accordingly:

$$SiO_2\ (l) + C\ (s) \rightarrow SiO\ (g) + CO(g) \quad (2)$$

$$SiO\ (g) + C\ (s) \rightarrow SiC\ (s) + CO(g) \quad (3)$$

$$SiO_2\ (l) + C\ (s) \rightarrow SiC\ (s) + 2CO(g) \quad (4)$$

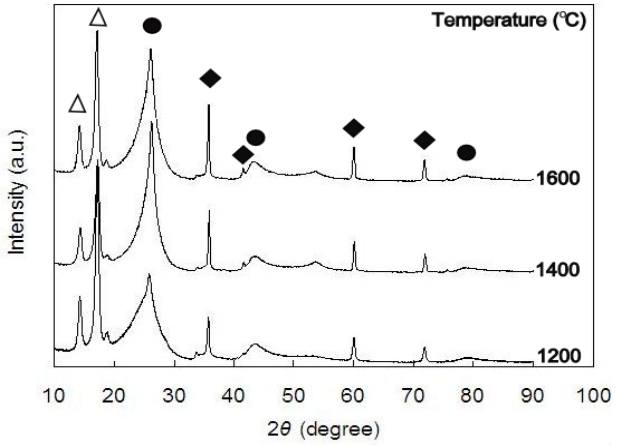

Figure 3. X-ray diffraction patterns of composites of SiC/SiO_2/C at different reaction temperatures. (●) C, (◆) β-SiC, (△) SiO_2.

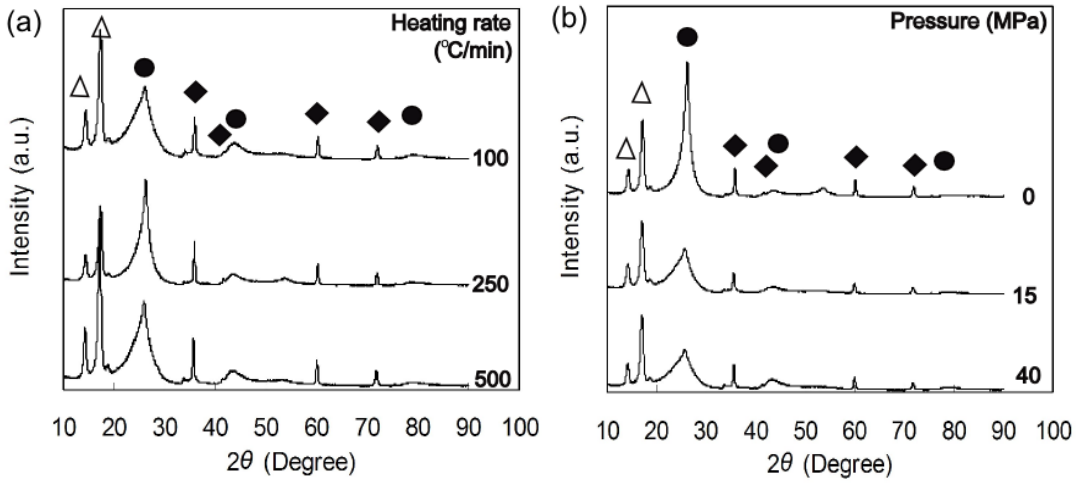

Figure 4. X-ray diffraction patterns of composites of SiC/SiO_2/C prepared at 1400°C with different (a) heating rates and (a) pressures. (●) C, (◆) β-SiC, (△) SiO_2.

SiO_2 in the liquid form was reacted with carbonized wood at interface to produce β-SiC. Meanwhile in the gas form, SiO penetrated into the interior of carbonized wood particles to form β-SiC. The reaction between SiO_2 in liquid phase and carbonized wood were also produced SiO and CO in gas phase. Some of SiO_2 and carbonized wood were still remained in the composites as shown in Figure 3. Our previous study found that the chemical compositions in the composites were SiC (0.3%), SiO_2 (4.1%) and C (85.6%) (Sulistyo *et al*. 2010).

Formation of SiC rod

A large number of rods were found on the surface of lumens and empty spaces between particles in composites of SiC/SiO_2/C as shown in the SEM image in Figure 5(a). The SiC rods were grown via a vapor-liquid-solid mechanism which was discussed in previous papers (Hata *et al*. 2005; Vyshnyakova *et al*. 2006; Cheung and Ng 2007). During the heat treatment, chemical reactions occurred between gaseous SiO and CO providing transport for the carbon and silicon needed for the growth of the SiC rods. The reaction that may occur to obtain SiC rods is as follows (Gao *et al*. 2002).

$$SiO\ (g) + 3CO\ (g) \rightarrow SiC\ (s) + 2CO_2\ (g) \qquad (5)$$

The SiO gas was produced by the reaction between SiO_2 (in liquid phase) and carbonized wood as discussed previously.

Figure 5(b) shows the Raman spectra of the rod body. A single peak appears at around 783~794 cm^{-1} in the Raman spectra corresponding to the transverse optic (TO) phonon mode of cubic β-SiC (Nakashima and Harima 1997; Rohmfeld *et al*. 1999; Shiryaev *et al*. 2008). It shows that the body of the rods contained β-SiC crystal. The strong and narrow TO peak with a width of 13 cm^{-1} in the Raman spectra indicated that SiC rods are well crystalline.

SiC rods Formation at Different Temperatures

Figure 6 shows that the SEM images of composites of SiC/SiO_2/C which were prepared at temperatures of 1200, 1400 and 1600°C. SiC rods exhibiting different morphologies were grown in all composites. Only the morphology and dimension of SiC rods could be observed. The SiC rods in the composites prepared at 1200 and 1400°C exhibited a straight structure with smooth surfaces. Meanwhile, the SiC rods in that of prepared at 1600°C exhibited a camelback-type structure, as shown in Figure 6(c). The reaction temperature also determined the length and diameter of SiC rods growth, as shown in Figure 7(a-b). The length and diameter of SiC rods increased with the increase of reaction temperature. The reaction temperature at 1600°C provided a greater activation energy which was needed to grow long and big diameter of SiC rods (Belmonte *et.al*. 1996). It was difficult to determine the yield of SiC rods in all composites.

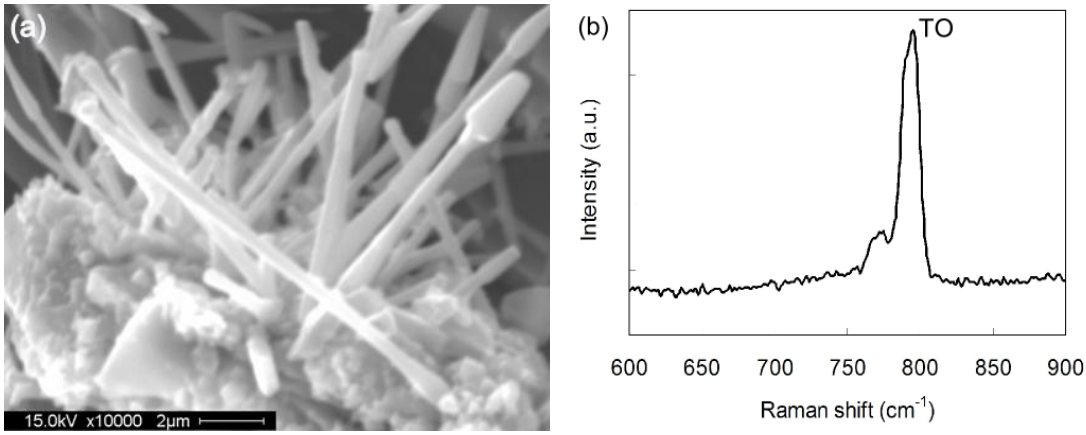

Figure 5. (a) A SEM image of SiC rods grown in the surface of the composite; (b) a single peak of transverse optic (TO) of Raman spectra in the range of 600-900 cm^{-1}.

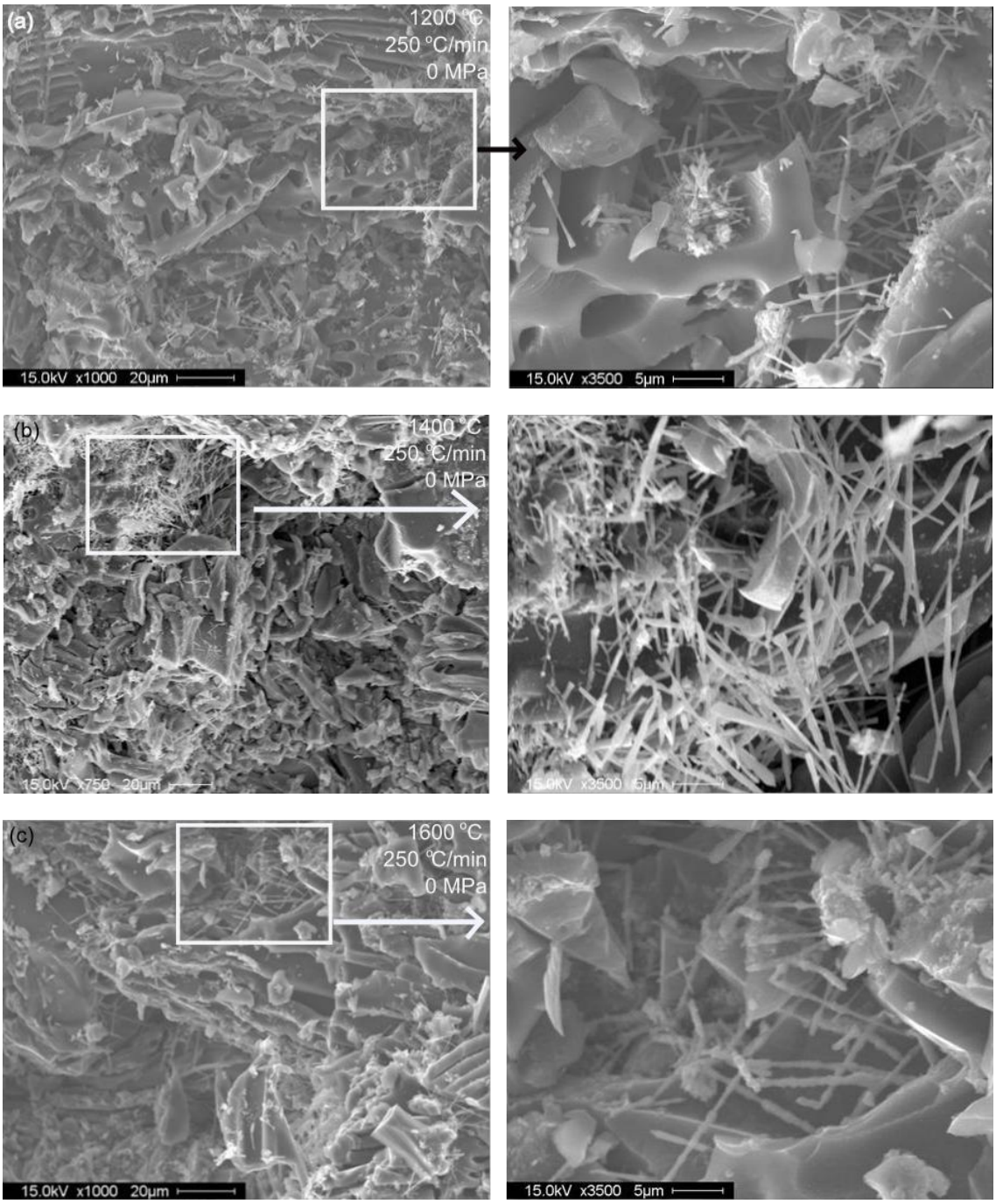

Figure 6. SEM images of SiC rod formation in composites of SiC/SiO_2/C prepared at temperatures of (a) 1200, (b) 1400 and (c) 1600°C with a heating rate of 250°C/min and without a pressure (0 MPa). The right images are the higher magnification of the square areas in the left images.

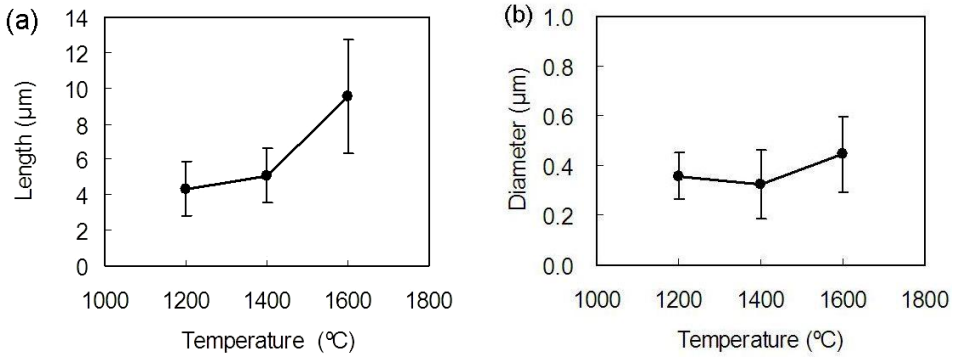

Figure 7. (a) The length and (b) diameter of SiC rod growth in composites of SiC/SiO_2/C prepared at different reaction temperatures with a heating rate of 250°C/min and without a pressure (0 MPa).

SiC rods Formation at Different Heating Rates

Figure 8 shows the SiC rods formation in composites of SiC/SiO_2/C at different heating rates. Both the heat treatment with rates of 100 and 500°C/min up to 1400°C determined the morphology of SiC rods which exhibited a camelback-type structure. Meanwhile the heat treatment with a rate of 250°C/min up to 1400°C could grow a straight-type structure of rods, as shown in Figure 6(b). Different heating rates also affected the size of SiC rods growth, as shown in Figure 9. However the diameter of SiC rods was difficult to be controlled by maintaining the heating rates. Heating rate of 500°C/min determined the longest SiC rods grown in composites of SiC/SiO_2/C. A fast heating rate causes the reaction temperature of 1400°C is able to be obtained in a short time. As a result, longer SiC rods growth is possible to be obtained.

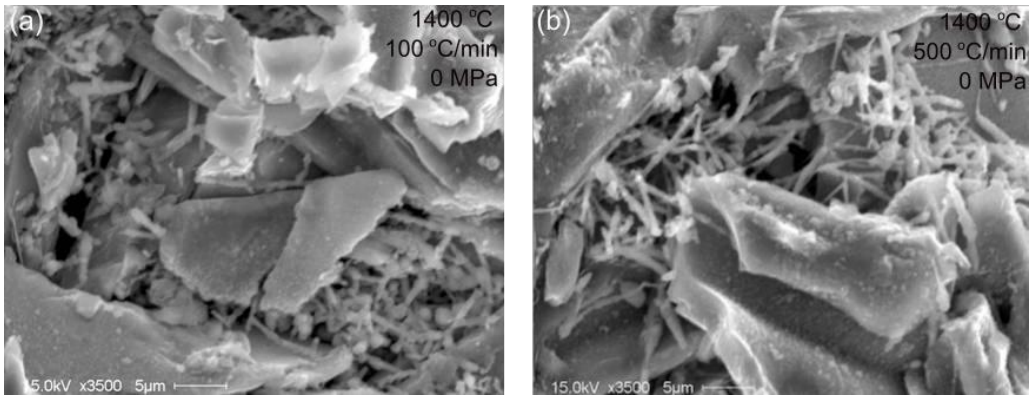

Figure 8. SEM images of SiC rod formation in composites of SiC/SiO_2/C prepared with heating rates of (a) 100 and (b) 500°C/min up to a temperature of 1400°C and without a pressure (0 MPa).

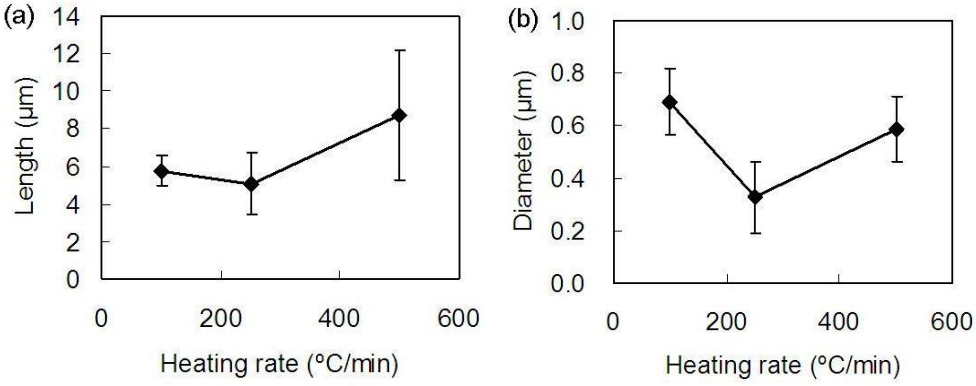

Figure 9. (a) The length and (b) diameter of SiC rod growth in composites of SiC/SiO_2/C prepared with different heating rates up to a temperature of 1400°C and without a pressure (0 MPa).

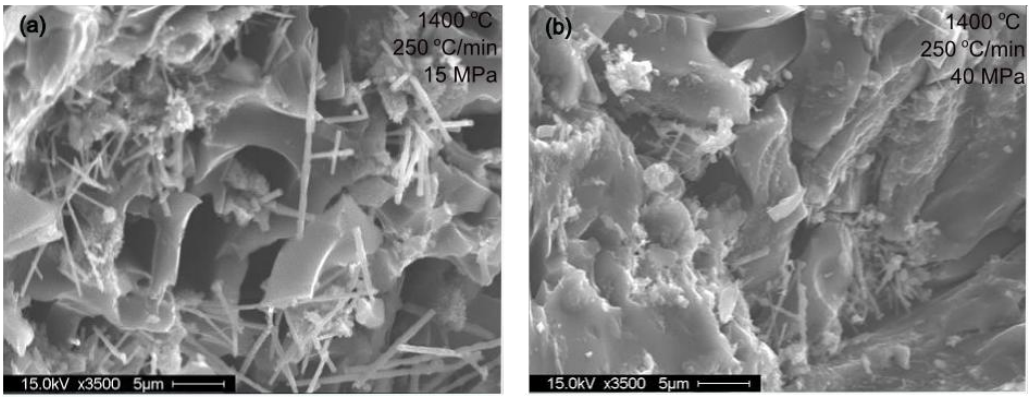

Figure 10. SEM images of SiC rods formation in composites of SiC/SiO_2/C prepared with pressures of (a) 15 and (b) 40 MPa at a temperature of 1400 °C and with a heating rate of 250 °C/min.

SiC rods Formation at Different Pressures

The increase of pressure from 0 to 15 MPa during the heat treatment at 1400°C increased the length and diameter of SiC rods grown, as shown in Figure 6(b), 10(a) and 11(a-b). The pressure of 15 MPa probably increased the saturation of SiO and CO vapors which were required for SiC rods growth. However the further increase of pressure to 40 MPa created lesser cavities in the composites, as shown in Figure 10(b). As a result, fewer SiC rods were grown in the composites prepared with a pressure of 40 MPa than those of 0 and 15 MPa.

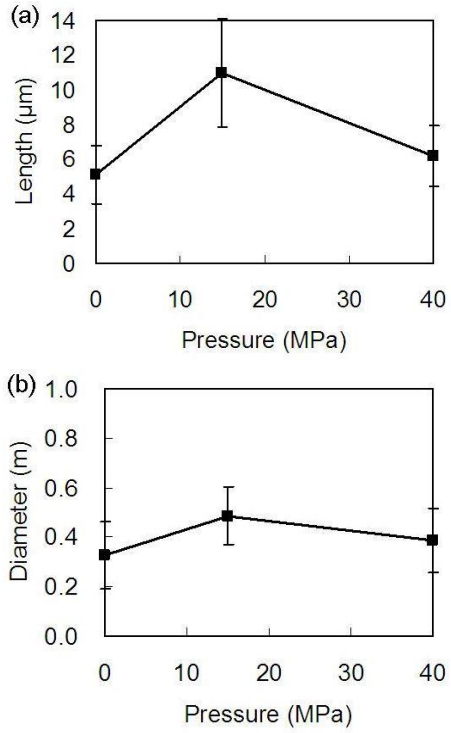

Figure 11. (a) The length and (b) diameter of SiC rod growth in composites of SiC/SiO_2/C prepared with different pressures at a temperature of 1400°C and with a heating rate of 250°C/min.

Conclusions

SiC rods were grown in composites of SiC/SiO_2/C from carbonized wood. Raman spectroscopy indicated that the SiC rods exhibited well crystalline. The morphology and dimensions of SiC rods were determined by temperature, heating rate and pressure. The SiC rods in the composites prepared at 1200 and 1400°C exhibited a straight structure with smooth surfaces. The increase of reaction temperature up to 1600°C increased the length and diameter of SiC rods which exhibited a camelback-type structure. Different heating rates only affected the length of SiC rods. Meanwhile the increase of pressure from 0 to 15 MPa at temperature of 1400°C increased the length and diameter of SiC rods.

References

Belmonte, T.; L. Bonnetain; J.L. Ginoux. 1996. Synthesis of Silicon Carbide Whisker Using the Vapour-Liquid-Solid Mechanism in a Silicon-Rich Droplet. Journal of Materials Science 31: 2367-2371.

Cheung, T.L.Y.; D.H.L. Ng. 2007. Conversion of Bamboo to Biomorphic Composites Containing Silica and Silicon Carbide Nanowires. Journal of American Ceramic Society 90: 559-564.

Fan, J.Y.; X.L. Wu; P.K. Chu. 2006. Low-dimensional SiC Nanostructures: Fabrication, Luminescence, and Electrical Properties. Progress in Materials Science 51:983-1031.

Fujisawa, M.; T. Hata; P. Bronsveld; V. Castro; F. Tanaka; H. Kikuchi; Y. Imamura. 2005. Thermoelectric Properties of SiC/C Composites from Wood Charcoal by Pulse Current Sintering. Journal of the European Ceramic Society 25: 2735-2738.

Gao, Y.H.; Y. Bando; K. Kurashima; T. Sato. 2001. The Microstructural Analysis of SiC Nanorods Synthesized through Carbothermal Reduction. Scripta Materials 44: 1941-1944.

Gao, Y.H.; Y. Bando; K. Kurashima; T. Sato. 2002. SiC Nanorods Prepared from SiO and Activated Carbon. Journal of Materials Science 37: 2023-2029.

Hata, T.; V Castro; M. Fujisawa; Y. Imamura; S. Bonnamy; P. Bronsveld; H. Kikuchi. 2005. Formation of Silicon Carbide Nanorods from Wood Based Carbons. Fullerene, Nanotube and Carbon Nanostructure 13: 107-113.

Klett, J.W.; A.D. McMillan; N.C. Gallego; C.A. Walls. 2004. The Role of Structure on the Thermal Properties of Graphitic Foam. Journal of Materials Science 39: 3659-3676.

Li Z.Q.; C.J. Lu; Z.P. Xia; Y. Zhou; Z. Luo. 2007. X-ray Diffraction Patterns of Graphite and Turbostratic Carbon. Carbon 45: 1686-1695.

Nakashima, S.; H. Harima. 1997. Raman Investigation of SiC Polytypes. Physica Status Solidi (a) 162: 39-64.

Pulido, L.; T. Hata; Y. Imamura; S. Ishihara; T. Kajimoto. 1998. Removal Mercury and Other Metals by Carbonized Wood Powder from Aqueous Solution of Their Salts. Journal of Wood Science 44: 237–243.

Rohmfeld, S.; S, Hundhausen; L. Ley. 1999. Influence of Stacking Disorder on the Raman Spectrum of 3C-SiC. Physics State Solid (b) 215: 115-119.

Senthil, K.; K. Yong. 2008. Enhanced Field Emission from Density-Controlled SiC Nanowires. Material Chemistry Physics 112: 88-93.

Shiryaev, A.A.; M. Wiedenbeck; V. Reutsky; V.B. Polyakov; N.N. Melnik; A.A. Lebedev; R. Yakimova. 2008. Isotopic Heterogeneity in Synthetic and Natural Silicon Carbide. Journal of Physics Chemistry Solid 69: 2492-2498.

Subyakto; T. Hata; S. Kawai; Y. Imamura; I. Ide. 2000. Anisotropic thermal properties of molded carbon phenolic spheres. Journal of Wood Science 46: 16-21.

Sulistyo, J.; T. Hata; M. Fujisawa; K. Hashimoto; Y. Imamura; T. Kawasaki. 2009. Anisotropic Thermal Conductivity of Three-layer Laminated Carbon-Graphite Composites from Carbonized Wood. Journal of Materials Science 44: 734-744.

Sulistyo, J.; T. Hata; H. Kitagawa; P. Bronsveld; M. Fujisawa; K. Hashimoto; Y. Imamura. 2010. Electrical and Thermal Conductivity of Porous SiC/SiO_2/C with Different Morphology from Carbonized Wood. Journal of Materials Science 45: 1107-1116.

Vyshnyakova, K.; G. Yushin; L. Pereselentseva; Y. Gogotsi. 2006. Formation of Porous SiC Ceramics by Pyrolysis of Wood Impregnated with Silica. International Journal of Applied Ceramics Technology 3: 485-490.

Wang, S.Y.; C.P. Hung. 2003. Electromagnetic Shielding Efficiency of the Electric Field of Charcoal from Six Wood Species. Journal of Wood Science 49: 450-454.

Zhu, S.; H. Xi; Q. Li; R. Wang. 2005. In Situ Growth of β-SiC Nanowires in Porous SiC Ceramic. Journal of American Ceramics Society 88: 2619-1612.

Joko Sulistyo and Sri Nugroho Marsoem
Department of Forest Products Technology,
Faculty of Forestry, Universitas Gadjah Mada, Yogyakarta
Tel. : 0274 - 550541
Fax. : 0274 - 550543
E-mail : jsulistyo@ugm.ac.id

Toshimitsu Hata
Research Institute for Sustainable Humanosphere,
Uji Campus - Kyoto University,
Gokasho, Uji, Kyoto 611-0011 JAPAN
Tel. : +81-774-38-3601
Fax. : +81-774-38-3600
E-mail : hata@rish.kyoto-u.ac.jp